Energy Conversion and Management 122 (2016) 411–418

Contents lists available at ScienceDirect

Energy Conversion and Management

journal homepage: www.elsevier.com/locate/enconman

# Statistical modeling/optimization and process intensification of microwave-assisted acidified oil esterification

Lingling Ma [a], Enmin Lv [a], Lixiong Du [a], Jie Lu [b,*], Jincheng Ding [a,*]

[a] College of Chemical Engineering, Shandong University of Technology, 12 Zhangzhou Road, Zibo, Shandong 255049, China
[b] Department of Resources and Environmental Engineering, Shandong University of Technology, 12 Zhangzhou Road, Zibo, Shandong 255049, China

ARTICLE INFO

*Article history:*
Received 26 March 2016
Received in revised form 17 May 2016
Accepted 1 June 2016

*Keywords:*
Microwave-assisted esterification
Response surface methodology
Artificial neural network
Molecular sieve 4Å
Vapor permeation

ABSTRACT

The esterification of acidified oil with ethanol under microwave radiation was modeled and optimized using response surface methodology (RSM) and artificial neural network (ANN). The impacts of mass ratio of ethanol to acidified oil, catalyst loading, microwave power and reaction time are evaluated by Box-Behnken design (BBD) of RSM and multi-layer perceptron (MLP) of ANN. RSM combined with BBD shows the optimal conditions as catalyst loading of 5.85 g, mass ratio of ethanol to acidified oil of 0.35 (20.0 g acidified oil), microwave power of 328 W and reaction time of 98.0 min with the free fatty acids (FFAs) conversion of 78.57%. Both of the models are fitted well with the experimental data, however, ANN exhibits better prediction accuracy than RSM based on the statistical analyses. Furthermore, membrane vapor permeation and in-situ molecular sieve dehydration were investigated to enhance the esterification under the optimized conditions.



## 1. Introduction

Biodiesel has attracted considerable attention due to the fast depletion of fossil fuel and the ever-worsening pollution of environment [1,2]. Biodiesel can be synthesized via transesterification of triglycerides (TGs) or esterification of free fatty acids (FFAs) [3]. In particular, biodiesel has advantages over petroleum-based diesel fuel such as higher cetane numbers, less smoke and particulates, lower hydrocarbon and carbon monoxide emissions and better performance in the engine lubricity [4,5]. However, the major challenge in biodiesel production is the high cost of raw materials [6]. In order to avoid the debate between food and fuel, biodiesel is mainly produced from the waste vegetable oils and animal fats in China. Low-cost feedstocks, such as acidified oil are generated by acidification of soapstock which is the by-product of the vegetable oil refining process. As a result, the use of acidified oil can reduce the cost of biodiesel. However, the acidified oil contains a lot of FFAs and cannot be directly processed with alkaline-catalysis technology [7]. To avoid saponification, FFAs in acidified oil is firstly esterified by acid-catalysts [8,9].

In the past two decades, microwave assisted esterification has been investigated as a powerful tool for process intensification [10]. The heat transfer in the traditional heating process occurs via conduction and convection. The significant drawback of the heating process is the dependence on the thermal conductivity, density and specific heat of materials [11]. Besides, the traditional heating requires long reaction time and the heat is not evenly distributed, leading to high energy consumption. Microwave irradiation for the esterification has the following advantages over the traditional heating process: (a) shorter reaction time, (b) more effective heat transfer, (c) lower molar ratio of alcohol to oil, (d) lower energy consumption and (e) environmental friendliness [12]. Microwaves are basically electromagnetic waves, a combination of a vertical magnetic field and an electrical wave, with wavelengths ranging from 1.0 mm to 1.0 m. Microwave irradiation follows two mechanisms, viz. dipolar rotation and ionic conduction [13]. In the esterification, the mixture contains oil, FFAs and alcohol, which has polar components. Hence, microwaves can heat the mixture to the required temperature efficiently and quickly. Liu et al. used aminophosphonic acid resin D418 to catalyze the microwave-assisted esterification [14]. However, there are few articles on modeling and optimizing the FFAs conversion via response surface methodology (RSM) and artificial neural network (ANN) under microwave radiation, especially when acidified oil is used.

The general approach of optimization is the one-factor-at-a-time method where one factor is changed while all the other parameters are kept constant. This conventional experimental

* Corresponding authors.
*E-mail addresses:* lujied@126.com, ljdjc@sdut.edu.cn (J. Lu), djclj@126.com, djclj@sdut.edu.cn (J. Ding).

http://dx.doi.org/10.1016/j.enconman.2016.06.001
0196-8904/

design is arduous, expensive and time consuming due to a large amount of experiments [15]. In addition, the traditional design ignores the interactions between the operating variables and does not fully represent the complete effects [16]. As a multivariate technique, RSM can assess the effects of independent variables and interactions among multiple variables. Besides, RSM can also generate a quadratic polynomial model [17]. Therefore, RSM is widely employed in the multivariable optimization field, including biodiesel production [18,19]. On the other hand, as a non-linear statistical technique, ANN modeling has been extensively applied to solve complex and ill-defined problems. ANN is able to handle incomplete data and execute fast predictions and generalizations [20–22]. The advantage of ANN over RSM is that ANN can solve nearly all kinds of non-linear systems, but RSM is limited by quadratic approximations [23]. Maran and Priya compared the performance of RSM and ANN in the in-situ transesterification process and demonstrated that the ANN model was more efficient than the RSM [24].

Generally, the esterification is characterized by thermodynamic limitation. The reaction is very slow and consumes a considerable amount of time to reach the equilibrium. Therefore, the method of removing water or using one reactant in excess is applied to shift the equilibrium. Co-distillation with entrainers (benzene or toluene) can remove water continuously, but this method is energy-consuming. Besides, these entrainers are toxic and harmful to the environment [25]. Vapor permeation (VP) is an environmental-friendly and energy-efficient membrane separation technique that has obvious advantages in the removal of water from the esterification mixture. In VP, the membrane is stable due to the indirect contact with liquid mixtures [26]. Ameri et al. used two different commercial membranes to selectively remove water in the esterification and found that a complete acid conversion was achieved [27]. Our previous work demonstrated the use of molecular sieve 4Å to remove water [15]. In this work, tubular NaA zeolite membrane and molecular sieve 4Å in spherical shape are studied by removing the side product of water under RSM optimized conditions.

To the best of our knowledge, the microwave assisted esterification from acidified oil is not reported wherein RSM and ANN are compared. Furthermore, the process intensification of microwave assisted esterification coupled with VP and molecular sieve dehydration under the optimized conditions has not been studied. Hence, this work is aimed to model and optimize the microwave assisted esterification from acidified oil using RSM and ANN. A four-factor three-level Box-Behnken design (BBD) and a multi-layer perceptron (MLP) were employed to predict the conversion of FFAs. In addition, both models were compared by the root mean square error (RMSE), coefficient of determination ($R^2$), absolute average deviation (AAD) and sum of squared error (SSE). Subsequently, two different dehydration approaches were studied under the optimized conditions to shift the equilibrium of the esterification.

## 2. Experimental

### 2.1. Materials and chemicals

The acidified oil was obtained from Zibo Jinxuan Resources and Environmental Technology Development Co., Ltd., China, and presented an acid value of 136.35 mg KOH/g (after filtration and drying). The sulfonated cation exchange resins (SCER) named CH-A was purchased from Shandong Dongda Chemical Industry (Group) Company, Zibo, China. Physicochemical properties and pretreatment method of SCER were described by Ma et al. [15]. Ethanol (purity > 99.7% w/w), 95.0% (v/v) ethanol and spherical molecular sieve 4Å were supplied from Yantai Shuangshuang Chemical Company, Yantai, China. The molecular sieve 4Å had an average pore size of 0.40 nm, an equivalent particle diameter of 2.67 mm, a bed porosity of 0.379, a bulk density of 770 kg/m$^3$ and a particle porosity of 0.615 [28]. As reported in our previous study, the molecular sieve 4Å was activated at 500.0 °C in a muffle furnace for 6.0 h [15]. The tubular NaA zeolite membrane (Φ12 × 450 mm, average pore size 0.41 nm) was purchased from Wuhan Zhihongsibo Chemical Technology Co., Ltd., Wuhan, China.

### 2.2. Fatty acid composition of feedstock

A small amount (about 1.0 μL) of acidified oil was analyzed using gas chromatography–mass spectrometry (GC–MS) (6890 N GC/5973 MS, Agilent Technologies) to determine the composition according to Feng et al. [29]. The acidified oil is composed of 43.15 wt% oleic, 35.19 wt% linoleic, 13.34 wt% palmitic, 5.09 wt% linolenic and 3.23 wt% stearic. The main components in the feedstock are oleic acid, linoleic acid and palmitic acid, which are consistent with the data from Cai et al. [30].

### 2.3. Experimental setup

The microwave reactor (XH-200A, Beijing Xianghu Science and Technology Development Co., Ltd., Beijing, China) is used as the source of microwave radiation for transferring the energy to the reactants directly. The system consists of a magnetic stirrer, a reflux condenser connected with an air-cooled condenser and an infrared temperature monitor. The stirring rate was 480 rpm [31]. A three-necked flask (250 ml) was fitted with the air-cooled condenser and the temperature sensor. Considering the security of electromagnetic tube, a beaker of water (100 ml) was settled in the reactor to absorb excess microwave radiation during each experiment.

### 2.4. Conversion of FFAs

The esterification was performed in a laboratory-scale microwave reactor at the reflux temperature of ethanol. For all experiments, 20.0 g of acidified oil was mixed with proportionate amounts of ethanol and SCER catalyst. Subsequently, the mixture was heated to the reflux temperature of alcohol by the microwave reactor under stirring. When the reaction was completed, the reaction mixture was cooled to room temperature and settled to separate the liquid phase (ethanol, unreacted acidified oil, fatty acid ethyl esters and water) and solid phase (SCER). The sample was taken out from the reaction system and treated by decompression distillation to remove excess ethanol and water to determine the acid value of reaction system so as to calculate conversion of FFAs. The FFAs content of the sample was determined using the titration method according to the China Standard-GB/T 5530-2005. The following mathematical equations are introduced to determine the acid value of product and the conversion of FFAs at a particular time:

$$S = (56.1 \times C_{KOH} \times V_{KOH})/m \quad (1)$$

where $S$ (mg $KOH$/g oil) is the acid value of sample, $C_{KOH}$ (mol/L) and $V_{KOH}$ (ml) are the concentration and volume of $KOH$ solution used for titration, respectively, and $m$ (g) is the mass of the analyzed sample.

$$X(\%) = \{(S_i - S_f)/S_i\} \times 100\% \quad (2)$$

where $X$ (%) is the conversion of FFAs, $S_i$ (mg $KOH$/g oil) is the initial acid value of acidified oil, and $S_f$ (mg $KOH$/g oil) is the final acid value of sample. The samples were measured at least three times. The final values were averaged and the errors were less than 5.0%.

### 2.5. Modeling of experiments by RSM

Design Expert 8.0 software was applied to generate the experimental design matrix. The independent variables include the catalyst loading ($X_1$), mass ratio of ethanol to acidified oil ($X_2$), microwave power ($X_3$) and reaction time ($X_4$). The range and level of independent factors are listed in Table 1. A four-factor three-level BBD was used to model and optimize the experiments, which formed 29 experimental runs (Table 2). The response of FFAs conversion ($Y$) is evaluated by a quadratic polynomial equation as follows:

$$Y = \beta_0 + \beta_1 X_1 + \beta_2 X_2 + \beta_3 X_3 + \beta_4 X_4 + \beta_{12} X_1 X_2 + \beta_{13} X_1 X_3 + \beta_{14} X_1 X_4 + \beta_{23} X_2 X_3 + \beta_{24} X_2 X_4 + \beta_{34} X_3 X_4 + \beta_{11} X_1^2 + \beta_{22} X_2^2 + \beta_{33} X_3^2 + \beta_{44} X_4^2 \quad (3)$$

where $Y$ is the predicted response for FFAs conversion, $\beta_0$ is the intercept coefficient, $\beta_1, \beta_2, \beta_3$ and $\beta_4$ are the linear coefficients, $\beta_{12}, \beta_{13}, \beta_{14}, \beta_{23}, \beta_{24}$ and $\beta_{34}$ are the interaction coefficients, $\beta_{11}, \beta_{22}, \beta_{33}$ and $\beta_{44}$ are the quadratic coefficients, and $X_1$, $X_2$, $X_3$ and $X_4$ are the uncoded independent variables.

**Table 1**
Experimental factors and their coded levels for the RSM modeling.

| Factors | Unit | Coded factor levels | |
|---|---|---|---|
| | | −1 | +1 |
| Catalyst loading ($X_1$) | g | 2 | 6 |
| Ethanol/oil mass ratio ($X_2$) | g/g | 0.25 | 1.75 |
| Microwave power ($X_3$) | W | 150 | 450 |
| Reaction time ($X_4$) | min | 10 | 110 |

**Table 2**
Experimental and predicted responses of RSM and ANN for the esterification of acidified oil.

| Run order | $X_1$ | $X_2$ | $X_3$ | $X_4$ | FFAs conversion (%) | | |
|---|---|---|---|---|---|---|---|
| | | | | | Observed | RSM | ANN |
| 1 | 2 | 1 | 450 | 60 | 39.08 | 42.67 | 39.41 |
| 2 | 4 | 0.25 | 300 | 10 | 53.42 | 55.89 | 53.32 |
| 3 | 4 | 1 | 300 | 60 | 54.74 | 54.81 | 54.6 |
| 4 | 6 | 1 | 300 | 10 | 67.94 | 66.71 | 67.40 |
| 5 | 4 | 1.75 | 300 | 10 | 52.77 | 51.12 | 52.69 |
| 6 | 4 | 1 | 300 | 60 | 54.52 | 54.81 | 54.34 |
| 7 | 2 | 1 | 150 | 60 | 47.05 | 47.01 | 47.14 |
| 8 | 4 | 1.75 | 150 | 60 | 54.19 | 55.33 | 54.06 |
| 9 | 4 | 1 | 300 | 60 | 55.27 | 54.81 | 55.11 |
| 10 | 6 | 1 | 300 | 110 | 73.14 | 75.08 | 72.45 |
| 11 | 6 | 1 | 150 | 60 | 66.47 | 64.58 | 65.98 |
| 12 | 4 | 1 | 450 | 10 | 43.16 | 44.52 | 43.37 |
| 13 | 4 | 1.75 | 450 | 60 | 62.48 | 61.95 | 62.11 |
| 14 | 4 | 0.25 | 150 | 60 | 65.59 | 63.78 | 65.12 |
| 15 | 4 | 1 | 150 | 10 | 44.90 | 48.23 | 45.05 |
| 16 | 4 | 0.25 | 450 | 60 | 60.41 | 56.93 | 60.10 |
| 17 | 4 | 0.25 | 300 | 110 | 70.00 | 73.35 | 69.40 |
| 18 | 4 | 1 | 450 | 110 | 71.32 | 68.63 | 70.68 |
| 19 | 6 | 1.75 | 300 | 60 | 69.66 | 69.96 | 69.07 |
| 20 | 2 | 1.75 | 300 | 60 | 52.56 | 54.06 | 52.48 |
| 21 | 6 | 1 | 450 | 60 | 66.94 | 68.69 | 66.43 |
| 22 | 2 | 1 | 300 | 110 | 66.54 | 65.43 | 66.04 |
| 23 | 4 | 1 | 300 | 60 | 54.63 | 54.81 | 54.49 |
| 24 | 4 | 1 | 150 | 110 | 65.87 | 65.14 | 65.39 |
| 25 | 4 | 1.75 | 300 | 110 | 75.45 | 74.68 | 74.69 |
| 26 | 2 | 0.25 | 300 | 60 | 49.55 | 49.88 | 49.56 |
| 27 | 6 | 0.25 | 300 | 60 | 78.44 | 77.57 | 77.59 |
| 28 | 2 | 1 | 300 | 10 | 37.06 | 32.78 | 37.45 |
| 29 | 4 | 1 | 300 | 60 | 54.90 | 54.81 | 54.75 |

### 2.6. Modeling of experiments by ANN

Matlab 7.11.0 (R2010b) was employed to model the process using ANN. The FFAs conversion was predicted by using an MLP neural network with back-propagation (BP) algorithm. A typical topology of MLP is given in Fig. 1 showing the three layers chosen for the esterification involving the input layer (4 neurons), hidden layer (7 neurons) and output layer (1 neuron). ANN also includes (a) data generator selection, (b) data generation, (c) data processing, (d) structure selection, (e) algorithm selection, (f) network training, (g) network testing and (h) network simulation and validation [24]. In this study, the hidden layer has a logistic sigmoid transfer function and the output layer has a purelin transfer function. The logistic sigmoid transfer and purelin transfer functions are as follows:

$$f(X) = 1/(1 + e^{-X}) \quad (4)$$

$$f(X) = X \quad (5)$$

### 2.7. Statistical analysis of results

The efficiencies of both models are quantified by comparing actual and predicted responses. The RMSE, $R^2$, AAD and SSE are calculated by the following equations:

$$RMSE = \left\{ \frac{1}{n} \sum_{i=1}^{n} (Y_p - Y_a)^2 \right\}^{1/2} \quad (6)$$

$$R^2 = 1 - \left\{ \left[ \sum_{i=1}^{n} (Y_p - Y_a)^2 \right] \Big/ \left[ \sum_{i=1}^{n} (Y_a - Y_m)^2 \right] \right\} \quad (7)$$

$$AAD = \left\{ \frac{1}{n} \sum_{i=1}^{n} [(Y_p - Y_a)/Y_a] \right\} \times 100 \quad (8)$$

$$SSE = \sum_{i=1}^{n} (Y_p - Y_a)^2 \quad (9)$$

$$MSE = \frac{1}{n} \sum_{i=1}^{n} (Y_p - Y_a)^2 \quad (10)$$

where $n$ is the number of experiments, $Y_p$ is the predicted values, $Y_a$ is the actual values and $Y_m$ is the average of the experimental values.

### 2.8. Microwave-assisted esterification coupled with the water adsorption

The esterification is a reversible reaction, therefore integration of reaction and separation can intensify the esterification. The integration of the VP process and molecular sieves into the microwave

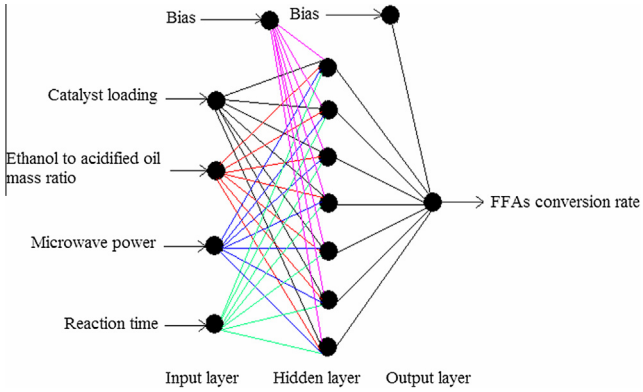


**Fig. 1.** Typical architecture of the developed ANN.

assisted esterification is attractive due to the opportunity to shift the conversion beyond the equilibrium by removing water selectively and continuously. In this work, these two intensification approaches are investigated under the RSM optimized conditions. The esterification of acidified oil with ethanol is described as follows:

$$R_1COOH(A) + CH_3CH_2OH(B) \xleftrightarrow{SCER} R_1COOCH_2CH_3(C) + H_2O(D) \quad (11)$$

where $A$ is FFAs, $B$ is ethanol, $C$ is fatty acid ethyl ester and $D$ is water.

## 3. Results and discussion

### 3.1. RSM modeling and optimization of microwave-assisted esterification

Experiments were carried out based on the BBD matrix and the average value was used for the data analysis. The experimental results of the RSM are presented in Table 2. Eq. (12) is the quadratic polynomial equation of model which relates the FFAs conversion to the process variables in terms of actual factors.

$$\begin{aligned} Y = {} & 42.30163 + 4.64858X_1 - 25.71570X_2 - 0.040209X_3 \\ & + 0.18940X_4 - 1.96500X_1X_2 + 7.03333 \times 10^{-3}X_1X_3 \\ & - 0.060700X_1X_4 + 0.029933X_2X_3 + 0.040667X_2X_4 \\ & + 2.39667 \times 10^{-4}X_3X_4 + 0.53704X_1^2 + 10.50563X_2^2 \\ & - 5.43593 \times 10^{-5}X_3^2 + 1.21627 \times 10^{-3}X_4^2 \end{aligned} \quad (12)$$

where $Y$ is the predicted response for the FFAs conversion, and $X_1$, $X_2$, $X_3$ and $X_4$ are the actual values of catalyst loading, mass ratio of ethanol to acidified oil, microwave power and reaction time, respectively. The positive coefficients ($X_1$, $X_4$, $X_1X_3$, $X_2X_3$, $X_2X_4$, $X_3X_4$, $X_1^2$, $X_2^2$ and $X_4^2$) present a favorable effect on the increase of FFAs conversion while the negative coefficients ($X_2$, $X_3$, $X_1X_2$, $X_1X_4$ and $X_3^2$) show an antagonistic effect on the increase of FFAs conversion.

Analysis of variance (ANOVA) for the FFAs conversion is used to determine the adequacy of the model. In order to test the hypotheses on the factors of the model, all variations are subdivided into component parts combined with specific sources of variations by ANOVA [32]. The statistical analysis results are displayed in Table 3.

**Table 3**
ANOVA results for the acidified oil esterification based on the RSM model.

| Source | Sum of squares | Degrees of freedom | Mean square | F-value | P-value prob > F |
|---|---|---|---|---|---|
| Model | 3271.28 | 14 | 233.33 | 30.80 | <0.0001 |
| $X_1$ | 1424.63 | 1 | 1424.63 | 187.77 | <0.0001 |
| $X_2$ | 8.84 | 1 | 8.84 | 1.17 | 0.2986 |
| $X_3$ | 0.039 | 1 | 0.039 | 5.079E−003 | 0.9442 |
| $X_4$ | 1262.19 | 1 | 1262.19 | 166.36 | <0.0001 |
| $X_1X_2$ | 34.75 | 1 | 34.75 | 4.58 | 0.0504 |
| $X_1X_3$ | 17.81 | 1 | 17.81 | 2.35 | 0.1478 |
| $X_1X_4$ | 147.38 | 1 | 147.38 | 19.42 | 0.0006 |
| $X_2X_3$ | 45.36 | 1 | 45.36 | 5.98 | 0.0283 |
| $X_2X_4$ | 9.30 | 1 | 9.30 | 1.23 | 0.2868 |
| $X_3X_4$ | 12.92 | 1 | 12.92 | 1.70 | 0.2129 |
| $X_1^2$ | 29.93 | 1 | 29.93 | 3.95 | 0.0669 |
| $X_2^2$ | 226.52 | 1 | 226.52 | 29.86 | <0.0001 |
| $X_3^2$ | 9.70 | 1 | 9.70 | 1.28 | 0.2771 |
| $X_4^2$ | 59.97 | 1 | 59.97 | 7.90 | 0.0139 |
| Residual | 106.22 | 14 | 7.59 | | |
| Lack of fit | 105.88 | 10 | 10.59 | 124.17 | 0.0002 |
| Pure error | 0.34 | 4 | 0.085 | | |
| Cor total | 3377.50 | 28 | | | |

The significance of each term of Eq. (3) is assessed by its corresponding P-value. A P-value greater than 0.05 indicates the model is insignificant [24]. The regression is significant at the 95.0% confidence interval when the P-value is less than 0.05 [15]. As shown in Table 3, the proposed model is highly significant ($P < 0.0001$) and the linear terms of $X_1$ and $X_4$, interactive terms of $X_1X_4$ and $X_2X_3$ and quadratic terms of $X_2^2$ and $X_4^2$ are significant.

The Fisher F-test (F-value) is used to check the fitness of the developed model and the values are presented in Table 3. Generally, a higher F-value and a lower P-value imply a higher significance of the model terms. In this case, the F-value of 30.80 and P-value less than 0.0001 indicates that the quadratic model is highly significant. There is only a 0.01% chance that a "Model F-Value" this large can occur due to the noise. In Table 3, two linear terms ($X_1$, $X_4$) and one quadratic term ($X_2^2$) show comparatively large effects on the FFAs conversion (high F-values and low P-values).

The developed quadratic model is evaluated by the determination co-efficient ($R^2$), predicted determination co-efficient ($R_{pred}$), adjusted determination co-efficient ($R_{adj}$), signal to noise ratio (S/N) and co-efficient of variance (CV). The value of the determination co-efficient ($R^2 = 0.9686$) of the model implies that the developed model can explain 96.86% of the total variations. The predicted determination co-efficient ($R_{prep} = 0.8193$) is in reasonable agreement with the adjusted determination co-efficient ($R_{adj} = 0.9371$). The value of $R_{adj}$ is very high and is close to the $R^2$, confirming that the proposed model is highly significant. The value of S/N greater than 4 is desirable. In this study, the value of S/N is 22.61, showing that the model can be used to navigate the design space. Furthermore, a high reliability and a high degree of precision of the experiments are demonstrated by a low value of CV (4.68%).

Based on the ANOVA analysis, the effect of each term on the FFAs conversion involving the SSE is shown in Table 3. It can be calculated that the most significant effect is $X_1$ (43.31%), followed by $X_4$ (38.37%). The overall effect of linear terms on the response is 81.95%, and the overall effect of the quadratic terms is 9.91%. The interactive terms have a relatively small effect on the response compared to other terms (8.13%). The effect of the residual error on the response is very low (0.23%). Therefore, the ANOVA results are supportive of the developed model. In this study, the predicted optimum FFAs conversion is 78.57% at the catalyst loading of 5.85 g, mass ratio of ethanol to acidified oil of 0.35, microwave power of 328 W and reaction time of 98.0 min. In order to verify the model, the conversion of 77.63% was obtained under the optimized conditions, indicating that the model is valid.

### 3.2. Effect of experimental variables in the RSM modeling

The interactions between operating variables and FFAs conversion in the acidified oil esterification are elucidated in Fig. 2a–f. Since the model has four variables, six plots are formed and each plot has two targeted variables while the others are kept constant. The three-dimensional (3D) surface plot of FFAs conversion as a function of catalyst loading and mass ratio of ethanol to acidified oil is depicted in Fig. 2a. As observed, the conversion of FFAs increases with an increase in catalyst loading at different mass ratios of ethanol to acidified oil. It demonstrates that catalyst loading has a significant effect on the response as revealed by the low P-value and high F-value. Fig. 2b illustrates the 3D surface plot for the interaction between catalyst loading and microwave power on the conversion. It is observed that an increase in catalyst loading from 2.0 g to 6.0 g results in an increase in the conversion of FFAs. In other words, more active sites can be provided due to the increase of catalyst loading. Microwave power in the range of 250–450 W is beneficial to the FFAs conversion at high catalyst loadings. The relationship of catalyst loading and reaction time is

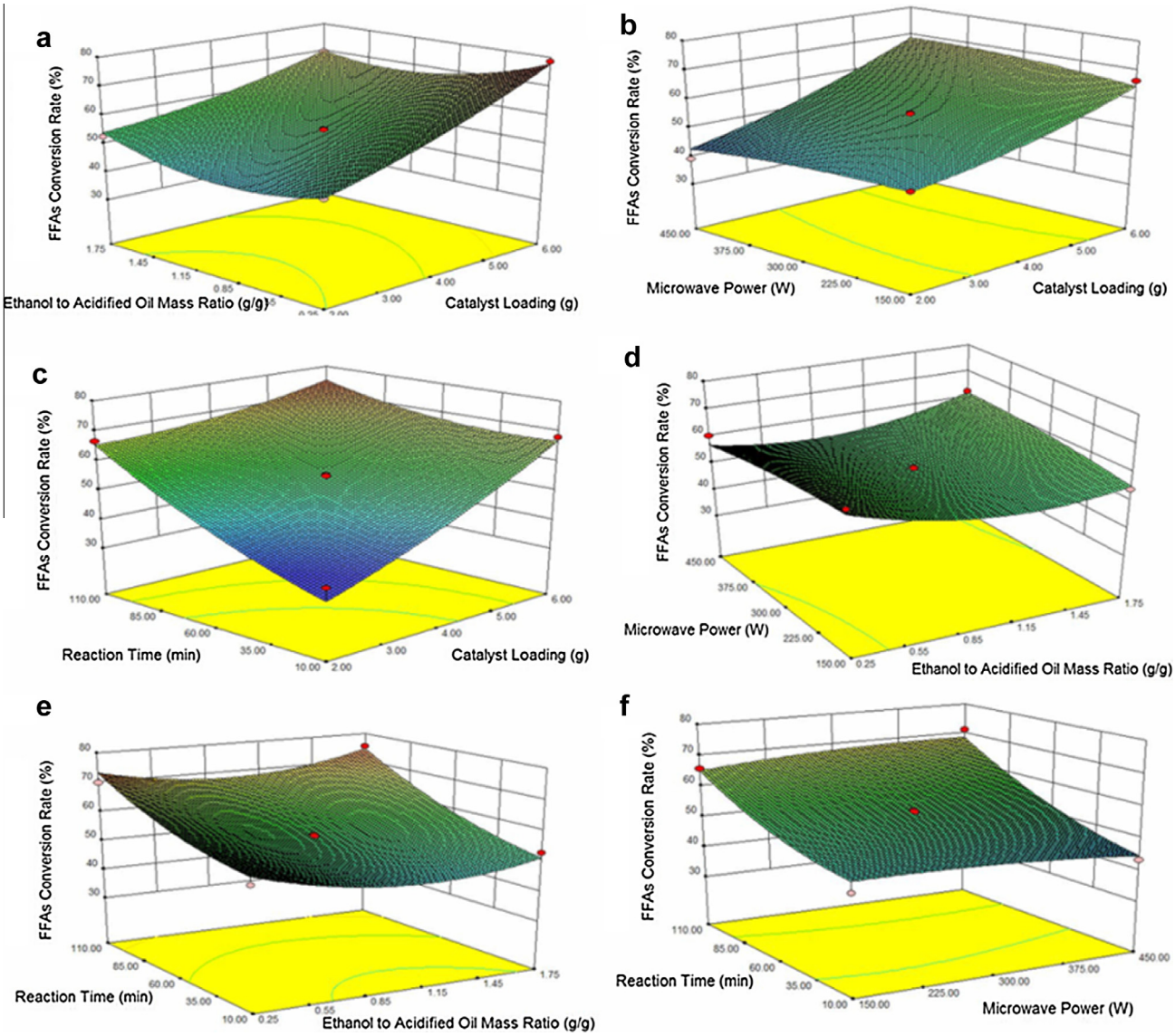


**Fig. 2.** Response surface plots for the FFAs conversion in the SCER catalyzed esterification.

presented in Fig. 2c. Both catalyst loading and reaction time influence the FFAs conversion significantly with the linear terms ($X_1$, $X_4$) and interactive term ($X_1X_4$) having profound impacts ($P < 0.05$) (Table 3). The curvature of the 3D surface indicates the significant interaction between catalyst loading and reaction time. Fig. 2d elucidates the interaction of ethanol to acidified oil mass ratio and microwave power. High FFAs conversions are favored by mass ratio and microwave power within the ranges of 0.25–0.55 g/g and 150–375 W and 1.30–1.75 g/g and 250–450 W, respectively. The relationship of ethanol to acidified oil mass ratio and reaction time is shown in Fig. 2e. Low conversion is observed at short reaction time and medium mass ratio. Namely, the conversion increases when the reaction time increases within a given range. However, microwave assisted esterification can reduce the reaction time effectively compared to the conventional heating method. Zhang et al. found that 97.40% conversion could be obtained at 90.0 min of operation by microwave assisted esterification, while 98.40% conversion was achieved at 8.0 h of operation by conventional heating method [31]. Fig. 2f demonstrates the interaction between microwave power and reaction time on the response. It can be seen that at the lowest microwave power, i.e. 150 W, an increase in reaction time will render higher conversion, which is analogous to the response at all other microwave powers up to the maximum, i.e. 450 W. In a similar manner, it can be observed that microwave power has little effect on the response at the constant reaction time.

### *3.3. ANN modeling and optimization of microwave-assisted esterification*

In ANN modeling, selecting the appropriate number of neurons in the hidden layer is important for developing suitable ANN model to predict the FFAs conversion. On the one hand, too many neurons can cause the over-fitting of the data, which can lead to the failure of network in relating the patterns. On the other hand, insufficient neurons can cause under-fitting of the data [33]. The obtained experimental data sets are divided into three subsets as training (70% of the experimental data sets), testing (15% of the experimental data sets) and validation (15% of the experimental data sets). In the training subset, these data are presented to the network during training, and the network is adjusted according to its error. In the testing subset, these data have no effect on training and so provide

an independent measure of network performance during and after training. In the validation subset, these data are used to measure the network generalization and halt training when the generalization stops improving.

The sensitivity of the ANN model is evaluated from 1 to 10 neurons in the hidden layer for ten different networks. The MSE is the average squared difference between outputs and targets. Low MSE values are desirable and zero means no errors. The MSE from different number of neurons for the FFAs conversion are presented in Fig. 3. The minimum MSE is obtained with 7 neurons in the hidden layer by closer observation. Therefore, the topology, i.e. 4–7–1, which has 7 neurons as the optimum, is used due to the minimum MSE value. In order to compare the regressions from experimental data and ANN predicted data, the scatter diagrams of training, validation and testing are shown in Fig. 4. Regression values (R) represents the correlation between outputs and targets. An R value of 1.0 means a close relationship and 0 indicates a random relationship. The scatter of points around the 45° line signifies that the ANN model has an excellent compatibility between targets (experimental data) and outputs (predicted data). From Fig. 4, it is manifested that the neural network has efficient approximated experimental values. The R values of training and all of data sets are 0.9966 and 0.9714, respectively. Evidently, the ANN model shows a good prediction capability of target values.

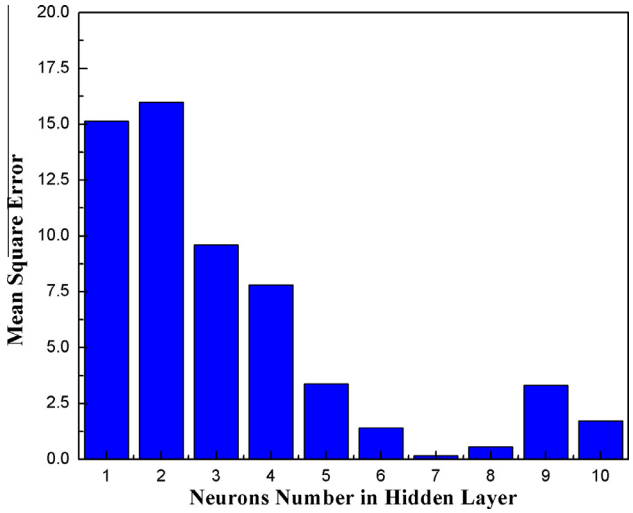


**Fig. 3.** The values of MSE for different number of neurons in the hidden layer.

### 3.4. Performance evaluation of RSM and ANN modeling

The efficiencies of both models are examined by comparing actual responses and predicted responses. The RMSE for BBD and ANN models are found to be 1.9138 and 0.4200, respectively. These results illustrate that the ANN model has a lower deviation than the BBD. The values of $R^2$ for both models are found to be 0.9675 (BBD) and 0.9984 (ANN), respectively. The AAD values for BBD and ANN are 2.7562% and 0.5619%, respectively. At the same time the SSE for both models are 106.2115 (BBD) and 5.1152 (ANN), respectively. These results reveal that the two optimization tools are fitted well with the observation data. However, the ANN model shows better predictive capability and data fitting than the BBD. This may be attributed to the non-linearity of ANN [34]. In addition, the distribution of residual errors of both models is shown in Fig. 5. Compared with the BBD, the residual values of ANN are relatively small. Hence, ANN shows superior prediction over RSM based on BBD matrix.

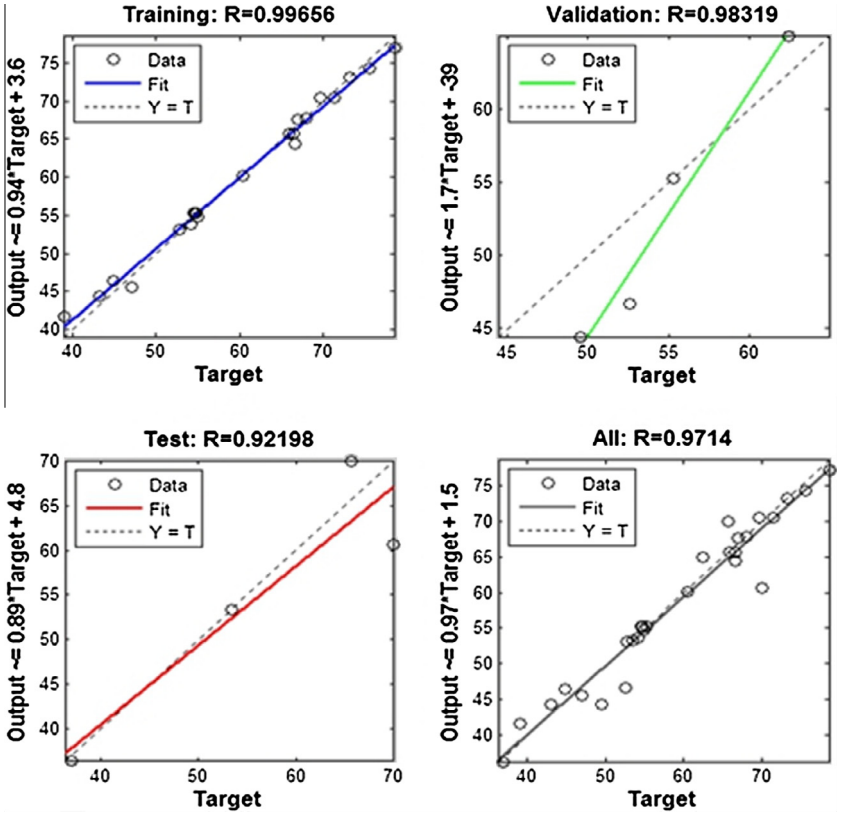


**Fig. 4.** The scatter diagrams of training, validation and testing and all prediction set for the ANN model.

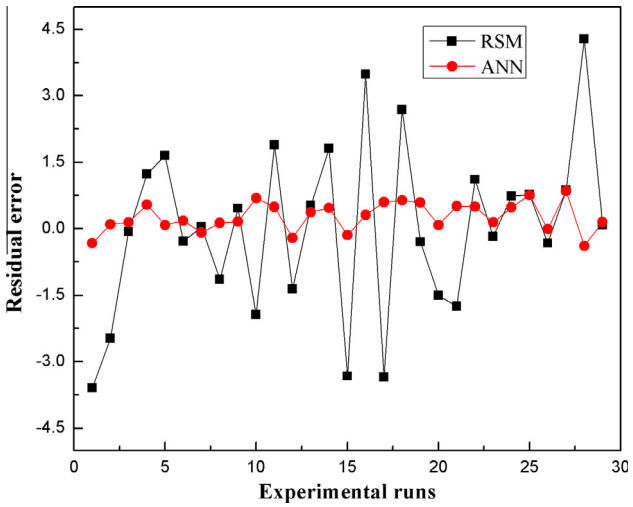


**Fig. 5.** The distribution of residual errors between experimental and predicted value by RSM and ANN.

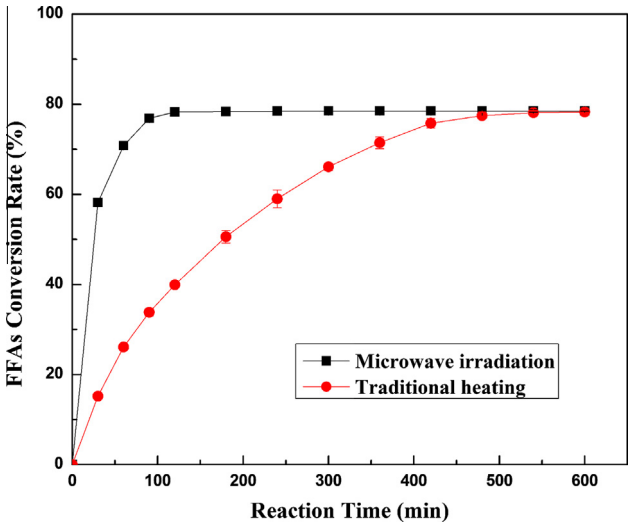


**Fig. 7.** Comparison of microwave assisted and traditional heating esterification under selected reaction conditions such as the catalyst loading of 5.0 g, mass ratio of ethanol to acidified oil of 1.0 and reaction time of 0.0–600.0 min. The error bars indicate the standard deviation of the mean.

### 3.5. Microwave-assisted esterification coupled with dehydration

The effects of using tubular NaA zeolite membrane and spherical molecular sieve 4Å for the reaction mixture dehydration on the FFAs conversion at the reflux temperature of ethanol were investigated under the RSM optimized conditions with microwave radiation. The experimental set-up is given in Fig. 6. The tubular membrane is installed in an empty distillation column connected with a vacuum pump. The permeating product is collected by using two liquid nitrogen traps. The spherical molecular sieve (100.0 g) is loaded in the empty distillation column in the same way.

Integration of reaction and separation could intensify the reversible esterification. Since the characteristic narrow structural pore openings can enable the only adsorption of smaller particles like water ($2.6 \times 10^{-10}$ m) and exclude adsorption of ethanol ($4.4 \times 10^{-10}$ m), tubular NaA zeolite membrane ($4.1 \times 10^{-10}$ m) and spherical molecular sieve 4Å ($4 \times 10^{-10}$ m) are selected for dehydration. The adsorption of ethanol could be negligible due to the large molecular size. In the case of using tubular NaA zeolite membrane, a high FFAs conversion of 97.11% is obtained. By coupling with VP, membrane dehydration improves the conversion of FFAs by 19.48%. Therefore, membrane separation is effective to overcome the chemical equilibrium limitation by removing water. Furthermore, by in-situ water removal using spherical molecular sieve 4Å, the conversion of FFAs increases from 77.63 to 95.99% under the RSM optimized conditions. Based on these results, it is concluded that these two dehydration methods are effective in removing or adsorbing the water during the esterification and increasing conversion of FFAs by shifting the equilibrium.

### 3.6. Comparison of microwave-assisted and traditional heating esterification

The esterification of acidified oil with ethanol over SCER is conducted by microwave and traditional heating under selected reaction conditions (catalyst loading of 5.0 g, mass ratio of ethanol to acidified oil of 1.0 with the acidified oil amount of 20.0 g and reaction time of 0.0–600.0 min), and the results are depicted in Fig. 7. As shown in Fig. 7, it takes 120.0 min to attain around 78.0% conversion of FFAs under 300 W microwave heating, while it takes about 540.0 min to reach about the same conversion by traditional heating. These results strongly evidence that microwave assisted esterification can offer a rapid route to produce fatty acid ethyl

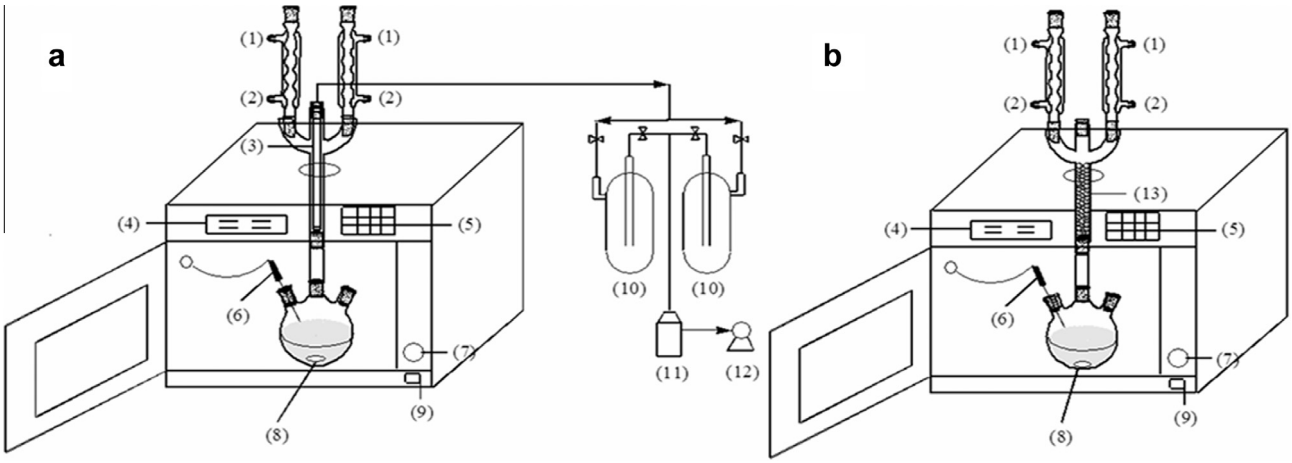


**Fig. 6.** Schematic diagram of the apparatus for intensified esterification under microwave radiation by (a) membrane vapor permeation and (b) in-situ molecular sieve dehydration, (1) cooling water (out), (2) cooling water (in), (3) tubular NaA zeolite membrane, (4) display screen, (5) control panel, (6) thermocouple, (7) magnetic controller, (8) magnetic stirrer bar, (9) mains switch, (10) cold traps, (11) buffer bottle, (12) vacuum pump, (13) spherical molecular sieve.

ester due to the short reaction time as described by Liu and Zhang et al. [14,31].

## 4. Conclusions

In this study, microwave assisted esterification from acidified oil was evaluated and modeled by RSM and ANN. The performance and predictive capabilities of RSM based on the BBD matrix and ANN were compared statistically. Based on the values of RMSE, $R^2$, AAD and SSE, both models are able to predict the experimental data, but ANN is superior over BBD. Furthermore, tubular NaA zeolite membrane and spherical molecular sieve 4Å were used to remove water selectively and continuously under the RSM optimized conditions. These two dehydration approaches improved the FFAs conversion by 20.0% approximately. Therefore, membrane VP and in-situ molecular sieve dehydration are feasible and effective to enhance the esterification under microwave irradiation.

## Acknowledgments

The authors acknowledge the support from the Natural Science Foundation of Shandong Province, China (Grant Nos. ZR2013BL010 and ZR2015EL044), the Research Excellence Award of Shandong University of Technology and the Zibo Technology Research and Development Program of China (Grant No. 2013GG04110). The authors also wish to express their thanks to Zibo Jinxuan Resources and Environmental Technology Development Co., Ltd, China, for their sincere help during this work.

## References

[1] Xie WL, Fan ML. Immobilization of tetramethylguanidine on mesoporous SBA-15 silica: a heterogeneous basic catalyst for transesterification of soybean oil. Bioresour Technol 2013;139:388–92.
[2] Dharma S, Masjuki HH, Ong HC, Sebayang AH, Silitonga AS, Kusumo F, et al. Optimization of biodiesel production process for mixed *Jatropha curcas–Ceiba pentandra* biodiesel using response surface methodology. Energy Convers Manage 2016;115:178–90.
[3] Fauzi AHM, Amin NAS, Mat R. Esterification of oleic acid to biodiesel using magnetic ionic liquid: multi-objective optimization and kinetic study. Appl Energy 2014;114:809–18.
[4] Jiang YW, Lu J, Sun KA, Ma LL, Ding JC. Esterification of oleic acid with ethanol catalyzed by sulfonated cation exchange resin: experimental and kinetic studies. Energy Convers Manage 2013;76:980–5.
[5] Uprety BK, Chaiwong W, Ewelike C, Rakshit SK. Biodiesel production using heterogeneous catalysts including wood ash and the importance of enhancing byproduct glycerol purity. Energy Convers Manage 2016;115:191–9.
[6] Abidin SZ, Haigh KF, Saha B. Esterification of free fatty acids in used cooking oil using ion-exchange resins as catalysts: an efficient pretreatment method for biodiesel feedstock. Ind Eng Chem Res 2012;51:14653–64.
[7] Ding JC, He BQ, Li JX. Cation ion-exchange resin/polyethersulfone hybrid catalytic membrane for biodiesel production. J Biobased Mater Bioenerg 2011;5:85–91.
[8] Ding JC, Xia Z, Lu J. Esterification and deacidification of a waste cooking oil (TAN 68.81 mg KOH/g) for biodiesel production. Energies 2012;5:2683–91.
[9] Ma LL, Han Y, Sun KA, Lu J, Ding JC. Kinetic and thermodynamic studies of the esterification of acidified oil catalyzed by sulfonated cation exchange resin. J Energy Chem 2015;24(4):456–62.
[10] Patil NG, Benaskar F, Rebrov EV, Meuldijk J, Hulshof LA, Hessel V, et al. Scale-up of microwave assisted flow synthesis by transient processing through monomode cavities in series. Org Process Res Dev 2014;18(11):1400–7.
[11] Jaliliannosrati H, Amin NAS, Talebian-Kiakalaieh A, Noshadi I. Microwave assisted biodiesel production from *Jatropha curcas* L. seed by two-step in situ process: optimization using response surface methodology. Bioresour Technol 2013;136:565–73.
[12] Teixeira CB, Junior JVM, Macedo GA. Biocatalysis combined with physical technologies for development of a green biodiesel process. Renew Sustain Energy Rev 2014;33:333–43.
[13] Maddikeri GL, Pandit AB, Gogate PR. Intensification approaches for biodiesel synthesis from waste cooking oil: a review. Ind Eng Chem Res 2012;51:14610–28.
[14] Liu W, Yin P, Liu XG, Chen W, Chen H, Liu CP, et al. Microwave assisted esterification of free fatty acid over a heterogeneous catalyst for biodiesel production. Energy Convers Manage 2013;76:1009–14.
[15] Ma LL, Han Y, Sun KA, Lu J, Ding JC. Optimization of acidified oil esterification catalyzed by sulfonated cation exchange resin using response surface methodology. Energy Convers Manage 2015;98:46–53.
[16] Betiku E, Okunsolawo SS, Ajala SO, Odedele OS. Performance evaluation of artificial neural network coupled with generic algorithm and response surface methodology in modeling and optimization of biodiesel production process parameters from shea tree (Vitellaria paradoxa) nut butter. Renew Energy 2015;76:408–17.
[17] Talebian-Kiakalaieh A, Amin NAS, Zarei A, Noshadi I. Transesterification of waste cooking oil by heteropoly acid (HPA) catalyst: optimization and kinetic model. Appl Energy 2013;102:283–92.
[18] Dwivedi G, Sharma MP. Application of Box–Behnken design in optimization of biodiesel yield from Pongamia oil and its stability analysis. Fuel 2015;145:256–62.
[19] Raita M, Arnthong J, Champreda V, Laosiripojana N. Modification of magnetic nanoparticle lipase designs for biodiesel production from palm oil. Fuel Process Technol 2015;134:189–97.
[20] Chakraborty R, Sahu H. Intensification of biodiesel production from waste goat tallow using infrared radiation: process evaluation through response surface methodology and artificial neural network. Appl Energy 2014;114:827–36.
[21] Rajendra M, Jena PC, Raheman H. Prediction of optimized pretreatment process parameters for biodiesel production using ANN and GA. Fuel 2009;88:868–75.
[22] Betiku E, Omilakin OR, Ajala SO, Okeleye AA, Taiwo AE, Solomon BO. Mathematical modeling and process parameters optimization studies by artificial neural network and response surface methodology: a case of non-edible neem (Azadirachta indica) seed oil biodiesel synthesis. Energy 2014;72:266–73.
[23] Fauzi AHM, Amin NAS. Optimization of oleic acid esterification catalyzed by ionic liquid for green biodiesel synthesis. Energy Convers Manage 2013;76:818–27.
[24] Maran JP, Priya B. Comparison of response surface methodology and artificial neural network approach towards efficient ultrasound-assisted biodiesel production from muskmelon oil. Ultrason Sonochem 2015;23:192–200.
[25] Li WX, Liu WW, Xing WH, Xu NP. Esterification of acetic acid and n-propanol with vapor permeation using NaA zeolite membrane. Ind Eng Chem Res 2013;52:6336–42.
[26] Okamoto K, Yamamoto M, Noda S, Semoto T, Otoshi Y, Tanaka K, et al. Vapor-permeation-aided esterification of oleic acid. Ind Eng Chem Res 1994;33:849–53.
[27] Ameri E, Moheb A, Roodpeyma S. Vapor-permeation-aided esterification of isopropanol/propionic acid using NaA and PERVAP 2201® membranes. Chem Eng J 2010;162:355–63.
[28] Gabruś E, Nastaj J, Tabero P, Aleksandrzak T. Experimental studies on 3A and 4A zeolite molecular sieves regeneration in TSA process: aliphatic alcohols dewatering–water desorption. Chem Eng J 2015;259:232–42.
[29] Feng YH, He BQ, Cao YH, Li JX, Liu M, Yan F, et al. Biodiesel production using cation-exchange resin as heterogeneous catalyst. Bioresour Technol 2010;101:1518–21.
[30] Cai ZZ, Wang Y, Teng YL, Chong KM, Wang JW, Zhang JW, et al. A two-step biodiesel production process from waste cooking oil via recycling crude glycerol esterification catalyzed by alkali catalyst. Fuel Process Technol 2015;137:186–93.
[31] Zhang HL, Ding JC, Zhao ZD. Microwave assisted esterification of acidified oil from waste cooking oil by CERP/PES catalytic membrane for biodiesel production. Bioresour Technol 2012;123:72–7.
[32] Maran JP, Priya B, Manikandan S. Modeling and optimization of supercritical fluid extraction of anthocyanin and phenolic compounds from *Syzygium cumini* fruit pulp. J Food Sci Technol 2014;51:1938–46.
[33] Majdi A, Rezaei M. Prediction of unconfined compressive strength of rock surrounding a roadway using artificial neural network. Neural Comput Appl 2013;23:381–9.
[34] Desai KM, Survase SA, Saudagar PS, Lele SS, Singhal RS. Comparison of artificial neural network (ANN) and response surface methodology (RSM) in fermentation media optimization: case study of fermentative production of scleroglucan. Biochem Eng J 2008;41:266–73.